
WHEN TASK-SPECIFIC LEARNING OUTPERFORMS TRANSFER LEARNING: A BENCHMARK OF GENE AND EXPRESSION ENCODING STRATEGIES*

Igor Sadalski

Somite.ai

Boston, MA, USA

igor.sadalski@gmail.com

ABSTRACT

Single-cell foundational models have emerged as a powerful tool for learning generalizable cellular representations from large-scale data. Most models in this domain use transformer backbones, which require careful engineering of gene and expression encoding strategies, yet there is no consensus on which encoding techniques are effective. To address this gap, we take a fundamentally different approach: we test different encoding paradigms and systematically compare them by training models from scratch under controlled conditions. Our pretraining was scaled to 10 million cells across 100 diverse datasets, a tenfold increase compared to similar studies. We find that contrary to common assumptions, task-specific learned embeddings consistently outperform pretrained embeddings from large protein models like ESM-2 across all evaluation metrics. The best configuration (soft binning with learned embeddings) achieves superior performance on classification tasks and represents a substantial improvement over alternative configurations on SCIB metrics. Our work provides clear empirical guidance for model design decisions and establishes a systematic benchmark for evaluating encoding strategies in single-cell foundational models.

1 INTRODUCTION

A major driver in recent years has been to build an AI virtual cell, i.e., multi-scale, multi-modal neural network models that can represent and simulate cellular behaviour across diverse states (Bunne et al., 2024). Leading models promise to enable universal embeddings (Rosen et al., 2023), cross-species transfer (Pearce et al., 2025), multi-task transfer learning for downstream applications (Cui et al., 2024; Theodoris et al., 2023), and batch correction (Wang et al., 2021). While foundational models can be generated for different omics data types (e.g., protein, transcriptomics, tissues), here we focus on transcriptomic data. In this domain, most of the models (e.g. Cui et al. (2024); Adduri et al. (2025); Pearce et al. (2025)) use a transformer (Vaswani et al., 2017) backbone. Since transcriptomic data inherently consists of two pieces of information, gene identities and their expressions, architects of these models are faced with a design choice on how to encode this information into embeddings that transformers can process.

Different encoding strategies embody distinct assumptions about what information is most useful. For genes, task-specific patterns versus biological priors, for expression values, continuous precision versus discrete robustness. Figure 4 provides a schematic overview of representative encoding paradigms. For gene encoding, some models learn embeddings de novo to capture dataset-specific co-expression relationships (Cui et al., 2024), while others leverage transfer learning from pretrained protein language models such as ESM-2 (Lin et al., 2023; Adduri et al., 2025) to incorporate evolutionary biological knowledge. For expression encoding, strategies range from discretizing into bins for computational efficiency (Cui et al., 2024; Gandhi et al., 2025) to using continuous or soft binning via MLPs (Pearce et al., 2025; Ho et al., 2024; Adduri et al., 2025) or applying binning based on logarithmic transformation (Wang et al., 2021).

*in preparation for ICLR 2026, 2nd Workshop on Foundation Models for Science

We present a controlled benchmark that quantifies these methodologies using consistent model architecture and training procedures at a large scale. We overcome the limitations of previous work by scaling up the pretraining data tenfold to 10 million cells, increasing dataset diversity by using 100 different datasets, introducing new tokenization strategies such as log binning and raw embedding, and performing evaluation against the Tabula Sapiens v2 benchmark.

The main contributions of this work are:

- **Tenfold increase in scale of pretraining data** to 10 million cells across 100 diverse datasets.
- **Systematic evaluation of encoding strategies** comparing learned versus ESM-2 gene embeddings and four expression encoding methods (hard binning, soft binning, log binning, raw embedding).
- **Comprehensive benchmark evaluation** across batch correction, biological preservation, classification, and reconstruction metrics.

2 RELATED WORK

Limited scientific literature has addressed this problem. Most benchmarking efforts have focused on evaluating downstream applications, such as perturbation prediction (Ahmann-Eltze et al., 2024; Wenteler et al., 2024), using already pretrained models. In this work, we focus more on specific architectural choices and pretrain our models from scratch. A similar approach was taken in HEIMDALL (Haber et al., 2025), a modular tokenization framework, where authors tried to evaluate different encoding strategies. However, they pretrain their transformer model on only a few datasets with a total of 1 million cells. In comparison, regular transformer models in the field are trained on, e.g., 266 million cells (Gandhi et al., 2025) and hundreds of diverse datasets. Given improved transformer performance with data scale (Kaplan et al., 2020), we scale our pretraining to better align with the field’s standard practices.

3 METHODS

3.1 MODEL ARCHITECTURE AND TRAINING

We represent cells as bags of gene-expression pairs. Each cell i contains M_i genes with non-zero expression values, represented as a sequence of gene-expression pairs:

$$\mathcal{C}_i = ((g_{i,1}, x_{i,1}), \dots, (g_{i,M_i}, x_{i,M_i})) \quad (1)$$

where $g_{i,j}$ denotes the j -th gene identifier and $x_{i,j}$ denotes its corresponding expression value in cell i .

Prior to encoding, we normalize expression values for each cell to a constant total c_{norm} and apply log1p transformation:

$$\tilde{x}_{i,j} = \log \left(1 + \frac{x_{i,j}}{\sum_{k=1}^{M_i} x_{i,k}} \times c_{\text{norm}} \right) \quad (2)$$

where M_i is the number of genes in cell i , c_{norm} is a normalization constant (typically 10^4 or 10^6), and k indexes over all genes in cell i . This normalization step ensures consistent scaling across cells with varying sequencing depths.

Because transformers scale with the square of the size of the context window (number of inputs), we employ a sampling strategy to select a subset of genes for each cell. Let $S : \mathcal{C}_i \rightarrow \{(g_{i,j}, x_{i,j})\}_{j=1}^K$ be a sampling function that takes cell i and returns K gene-expression pairs, where $K = \min(\text{context_window}, M_i)$. During training, for datasets where the number of non-zero expressed genes exceeds the context window, we randomly sample K genes from all non-zero expressed genes in each cell:

$$\mathcal{S}_{\text{random}}^{(i)} = \text{RandomSample}(\{g_j : x_{i,j} > 0\}, K) \quad (3)$$

This approach ensures diverse gene representation across training examples while maintaining computational feasibility for large gene vocabularies.

The training objective is to predict masked expression values given the gene identities and unmasked expression context. To this end, we first compute embeddings for both gene identities and expression values. The gene embedding for each gene is obtained as:

$$\mathbf{e}_g^{(i,j)} = \text{enc}_g(g_{i,j}) \in \mathbb{R}^{d_g}, \quad (4)$$

where enc_g is the gene encoding function (detailed in Section 3.2), d_g is the gene embedding dimension, and $\mathbf{e}_g^{(i,j)} \in \mathbb{R}^{d_g}$ is the gene embedding vector. For expression values, we randomly mask a fraction p_{mask} of gene-expression pairs during training. The expression embedding is computed as:

$$\mathbf{e}_x^{(i,j)} = \begin{cases} \text{enc}_x(\tilde{x}_{i,j}) & \text{with probability } 1 - p_{\text{mask}} \\ \mathbf{m} & \text{with probability } p_{\text{mask}} \end{cases} \quad (5)$$

where enc_x is the expression encoding function (detailed in Section 3.3), $\mathbf{e}_x^{(i,j)} \in \mathbb{R}^{d_x}$ is the expression embedding vector, p_{mask} is the masking probability, and $\mathbf{m} \in \mathbb{R}^{d_x}$ is a learnable mask token with dimension d_x matching the expression embedding dimension.

The combined gene-expression embedding for the j -th gene in cell i is obtained by summing the gene and expression embeddings:

$$\mathbf{z}_0^{(i,j)} = \mathbf{e}_g^{(i,j)} + \mathbf{e}_x^{(i,j)} \quad (6)$$

where $\mathbf{z}_0^{(i,j)} \in \mathbb{R}^d$ is the combined embedding for gene j in cell i , and d is the model dimension (equal to both d_g and d_x). The combined embeddings for all K genes in cell i are concatenated together to form the input sequence for the model:

$$\mathbf{z}_0^{(i)} = [\mathbf{z}_0^{(i,1)}, \dots, \mathbf{z}_0^{(i,K)}] \quad (7)$$

where $\mathbf{z}_0^{(i)} \in \mathbb{R}^{K \times d}$ is the input sequence for cell i containing K gene embeddings. These combined embeddings are then passed through a transformer encoder. Grouping the gene-embeddings per cell and recursively applying the transformer layers, we obtain:

$$\mathbf{z}_l^{(i)} = f_{\text{transformer}}(\mathbf{z}_{l-1}^{(i)}) \quad (8)$$

where $f_{\text{transformer}}$ denotes a standard transformer encoder layer, $l \in \{1, \dots, n\}$ indexes the layers, and n is the total number of transformer layers.

The predicted expression value for the j -th gene in cell i is decoded from the final transformer layer output using a simple MLP:

$$\bar{x}_{i,j} = \text{MLP}(\mathbf{z}_n^{(i,j)}) \quad (9)$$

where $\mathbf{z}_n^{(i,j)} \in \mathbb{R}^d$ is the output embedding for gene j in cell i from the final transformer layer, and $\bar{x}_{i,j} \in \mathbb{R}$ is the predicted expression value. We optimize the model using mean squared error loss for reconstruction of masked gene expression values (Wang et al., 2021; Adduri et al., 2025; Ho et al., 2024; Cui et al., 2024):

$$\mathcal{L}_{i,j} = \frac{1}{|\mathcal{U}_{\text{unk}}|} \sum_{j \in \mathcal{U}_{\text{unk}}} (\tilde{x}_{i,j} - \bar{x}_{i,j})^2 \quad (10)$$

where $\mathcal{L}_{i,j}$ is the loss for gene j in cell i , \mathcal{U}_{unk} represents the set of masked gene indices, $\tilde{x}_{i,j}$ is the normalized true expression value, and $\bar{x}_{i,j}$ is the predicted expression value from Equation 9.

3.2 GENE ENCODING STRATEGIES

Learned encoding is obtained by passing the gene identifier through a learned embedding table (Cui et al., 2024; Gandhi et al., 2025). This approach allows the model to generate task-specific representations for each gene, enabling it to capture dataset-specific relationships.

$$\text{enc}_g^{\text{learned}}(g_{i,j}) = \text{Embedding}(g_{i,j}) \quad (11)$$

ESM-2 encoding uses precomputed embeddings retrieved from the ESM-2 (3B) model dictionary (Lin et al., 2023). STATE (Adduri et al., 2025) leverages this approach, using large pretrained protein language models to provide biologically-informed representations that are consistent across datasets and species, making it a strong choice for transfer learning and handling new or rare gene symbols. We project these embeddings through an MLP to match the model dimension.

$$\text{enc}_g^{\text{ESM-2}}(g_{i,j}) = \text{MLP}(\mathcal{E}(g_{i,j})) \quad (12)$$

where $\mathcal{E}(g_{i,j})$ denotes the precomputed ESM-2 embedding for gene identifier $g_{i,j}$, and MLP is a multi-layer perceptron that projects the embedding to the model dimension.

3.3 EXPRESSION ENCODING STRATEGIES

Raw expression encoding uses a simple MLP on normalized data. This approach preserves the full, continuous information from the expression measurement and is the most direct way to encode quantitative gene expression levels.

$$\text{enc}_x^{\text{raw}}(\tilde{x}_{i,j}) = \text{MLP}(\tilde{x}_{i,j}) \quad (13)$$

Hard binning encoding discretizes expression values into bins. This method groups expression levels into discrete intervals, trading off resolution for robustness and simplifying the input space (Cui et al., 2024; Gandhi et al., 2025).

$$b_{i,j} = \begin{cases} k, & \text{if } x_{i,j} > 0 \text{ and } x_{i,j} \in [\beta_k, \beta_{k+1}], \\ 0, & \text{if } x_{i,j} = 0, \end{cases} \quad (14)$$

where $b_{i,j}$ is the bin index for the expression value of gene j in cell i , k is the bin index, and β_k and β_{k+1} are the lower and upper boundaries of bin k , respectively. Expression embedding is obtained using an embedding layer:

$$\text{enc}_x^{\text{hard bin}}(x_{i,j}) = \text{Embedding}(b_{i,j}) \quad (15)$$

Log binning encoding compresses a wide dynamic range of expression values using a logarithmic transformation before discretizing. This approach can potentially mitigate the effects of outliers or skewed distributions. STATE (Adduri et al., 2025) uses this approach with ESM-2 embeddings, while scBERT (Wang et al., 2021) employs log binning with discrete tokenization.

$$b_{i,j} = \min(\lfloor \log_2(x_{i,j} + 1) \rfloor, B_{\max}) \quad (16)$$

where $b_{i,j}$ is the bin index for the expression value of gene j in cell i , and B_{\max} is the maximum bin index. Bins are embedded using an embedding layer:

$$\text{enc}_x^{\text{log bin}}(x_{i,j}) = \text{Embedding}(b_{i,j}) \quad (17)$$

Soft binning encoding uses a softmax over potential bins to allow fractional/bin-weighted expression, which can capture uncertainty and subtle intensity differences between expression values, making the encoding differentiable and potentially more expressive (Ho et al., 2024; Hao et al., 2024; Pearce et al., 2025).

$$\boldsymbol{\alpha}_x^{(i,j)} = \text{Softmax}(\mathbf{W}_{x,2} \text{LeakyReLU}(\mathbf{W}_{x,1} x_{i,j})) \quad (18)$$

where $\boldsymbol{\alpha}_x^{(i,j)}$ is a vector of bin weights for the expression value of gene j in cell i , $\mathbf{W}_{x,1}$ and $\mathbf{W}_{x,2}$ are learnable weight matrices, and LeakyReLU is the LeakyReLU activation function. The expression embedding is obtained by performing a soft lookup in the embedding table:

$$\text{enc}_x^{\text{soft bin}}(x_{i,j}) = \sum_{k=1}^b \alpha_{x,k}^{(i,j)} \mathbf{T}_k \quad (19)$$

where b is the number of bins, $\alpha_{x,k}^{(i,j)}$ is the k -th element of $\boldsymbol{\alpha}_x^{(i,j)}$, and \mathbf{T}_k is the k -th embedding vector in the embedding table \mathbf{T} .

4 EXPERIMENTS

4.1 DATASETS

Training data. We train our models on 101 diverse single-cell RNA sequencing datasets comprising over 10 million cells, randomly selected from the curated collection used to train the Transcriptformer model (Pearce et al., 2025). The datasets span diverse tissue types, experimental protocols, species, biological conditions, developmental stages, and disease states. See Appendix A for full details, including Table 2.

Evaluation data. We evaluate all models on 26 tissue-specific datasets from the Tabula Sapiens v2 benchmark (Tabula Sapiens Consortium et al., 2022), comprising 548,977 cells across diverse human tissues. This benchmark represents a standard evaluation protocol in the field and has been used to evaluate other foundational models (Pearce et al., 2025).

4.2 EVALUATION PROTOCOL

We evaluate model performance using standard single-cell benchmarks across four complementary dimensions Pearce et al. (2025); Luecken et al. (2022).

Batch correction metrics. To assess batch effect removal we use scib package (Luecken et al., 2022), we computed: Integration Local Inverse Simpson’s Index, which measures the diversity of batch labels in the local neighborhood of each cell to quantify batch mixing; Cell-type Local Inverse Simpson’s Index, which evaluates the preservation of biological structure by measuring the diversity of cell-type labels in the local neighborhood; Average Silhouette Width for batch, which measures how well batches are mixed globally using average silhouette width; and graph connectivity, which assesses whether cells sharing the same label form a fully connected subgraph in the k-nearest neighbors graph.

Biological preservation metrics. Similarly to batch correction metrics (also using scib package (Luecken et al., 2022)) we computed: Average Silhouette Width for label, which quantifies how well cells of the same cell type cluster together using average silhouette width computed over cell-type labels; Normalized Mutual Information, which measures the normalized mutual information between predicted clusters and true cell-type labels; Adjusted Rand Index, which computes the adjusted rand index between predicted clusters and true cell-type labels; isolated label F1 score, which evaluates the F1 score for cell types that are isolated in the embedding space; and isolated label silhouette, which measures the silhouette score for isolated cell types.

Cell type classification. To compute cell type classification performance, we extract cell embeddings from the model by mean-pooling gene embeddings from the final encoder layer (Pearce et al., 2025). We filter out cells with missing cell type annotations and remove cell types with fewer than 250 cells to ensure robust evaluation. We split the data into training and test sets using an 80/20 stratified split. We train a k-nearest neighbors classifier with $k = 10$ on the training set and evaluate performance on the held-out test set.

Reconstruction metrics. We evaluate reconstruction performance using Mean Squared Error on masked gene expression values, which directly measures the model’s ability to predict masked expression values during pretraining.

5 RESULTS

Figure 1 shows the trade-off between batch correction and biological preservation across all encoding configurations. Configurations in the upper right quadrant achieve the best balance of batch correction and biological preservation. Learned gene embeddings with soft binning consistently outperform other combinations, achieving superior batch mixing while preserving biological structure. On average, learned embeddings achieve a 29% relative improvement over ESM-2 embeddings on the combined SCIB metrics. The best configuration (soft binning with learned embeddings) achieves a SCIB score of 0.547, representing a 16% improvement over the second-best configuration (raw encoding with learned embeddings at 0.471). The performance gap between learned and ESM-2 embeddings is particularly pronounced, with learned embeddings showing more consistent perfor-

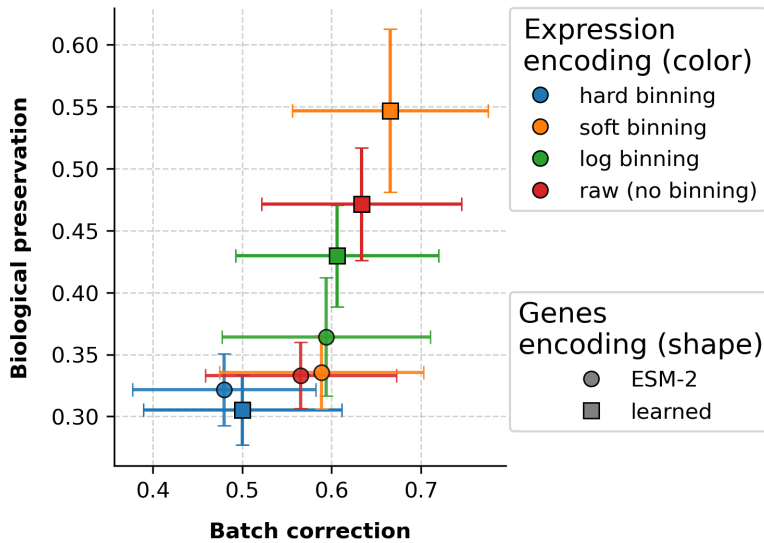


Figure 1: Performance comparison across encoding strategies on batch correction and biological preservation metrics. Each point represents a model configuration with error bars showing standard deviation across 26 datasets. X-axis: batch removal performance (mean of Integration Local Inverse Simpson’s Index, graph connectivity, Average Silhouette Width for batch). Y-axis: biology conservation performance (mean of Average Silhouette Width for label, Cell-type Local Inverse Simpson’s Index, Normalized Mutual Information, Adjusted Rand Index, isolated label F1 score, isolated label silhouette score). Colors indicate expression encoding strategies (hard binning, soft binning, log binning, raw expression); marker shapes indicate gene encoding strategies (learned embedding, ESM-2 embedding).

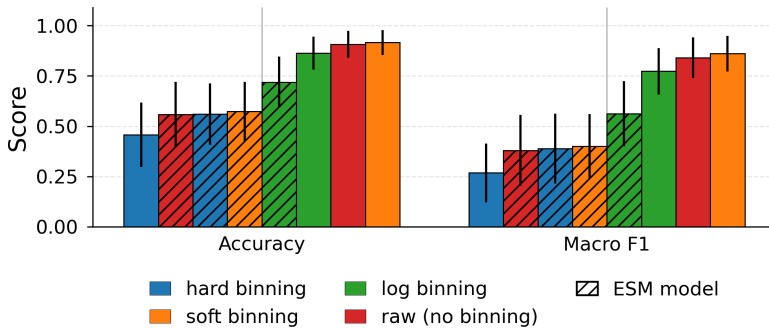


Figure 2: Cell type classification performance across encoding strategies. Bars show mean accuracy and macro F1 score with error bars indicating standard deviation across 26 datasets. Colors indicate expression encoding strategies (hard, soft, log, raw); hatching (///) indicates ESM-2 gene encoding. Configurations are sorted by accuracy in ascending order.

mance across tissue types. This pattern suggests that task-specific representations better capture the biological signal relevant for both batch correction and cell type preservation.

Figure 2 shows cell type classification performance measured by accuracy and macro F1 score. Learned gene embeddings consistently outperform ESM-2 embeddings across all expression encoding strategies, achieving 30% higher accuracy and 58% higher macro F1 score on average. The performance gap is most pronounced for hard and soft binning. Among expression encodings, soft binning achieves the best performance when combined with learned gene embeddings (91.6% accuracy, 86.0% macro F1), followed by raw encoding (90.7% accuracy, 84.0% macro F1), log binning

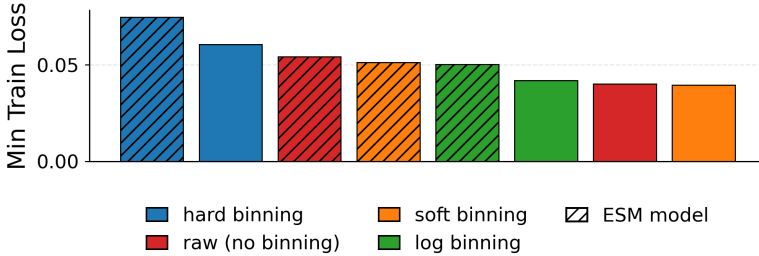


Figure 3: Minimum training loss achieved during pretraining for each model configuration. Bars are sorted by minimum loss in descending order. Colors indicate expression encoding strategies (hard, soft, log, raw); hatching (///) indicates ESM-2 gene encoding.

(86.3% accuracy, 77.3% macro F1), and hard binning (45.8% accuracy, 26.8% macro F1). Soft binning with learned embeddings shows a 92% improvement in macro F1 score over hard binning with learned embeddings, demonstrating the substantial benefit of differentiable expression encoding. The consistent outperformance of learned embeddings demonstrates that task-specific representations capture more relevant information for downstream classification tasks than transfer learning from protein language models.

Figure 3 shows the minimum training loss achieved during pretraining for each model configuration. Configurations with learned gene embeddings consistently achieve lower minimum training loss than ESM-2 configurations (0.046 vs 0.058 MSE on average, representing a 21% improvement), which aligns with the downstream performance results and suggests that the training instability observed with ESM-2 embeddings limits their effectiveness.

6 DISCUSSION

Our experiment reveal that, first, learned embeddings outperform ESM-2 embeddings and second, soft binning provides the optimal expression encoding strategy.

Learned gene embeddings outperform ESM-2 encoding. In principle, since there is an MLP layer from the ESM-2 embeddings to the model dimension, there shouldn’t be any significant difference between the model trained with ESM-2 embeddings and the model trained with learned embeddings. However, in practice we observed that the model trained with ESM-2 embeddings had a very unstable training process, with loss diverging before the training finished in all four cases. Quantitatively, learned embeddings achieve an average 39% relative improvement over ESM-2 embeddings across SCIB metrics, classification accuracy, and macro F1 score. The improvement is most dramatic for macro F1 score (58% improvement), followed by classification accuracy (30%) and SCIB metrics (29%). This substantial and consistent performance gap across all evaluation dimensions suggests that task-specific representations capture dataset-specific co-expression relationships that are more relevant for transcriptomic tasks than evolutionary protein-level information. Second, the gene vocabulary in single-cell data includes many non-coding genes, pseudogenes, and gene isoforms that are not well-represented in protein language models.

Soft binning has the best performance for expression encoding. Soft binning provides a balance between discrete and continuous representations. When combined with learned gene embeddings, soft binning achieves the best performance across all metrics: 91.6% classification accuracy and 86.0% macro F1 score, representing a 1% improvement over raw encoding and a 6% improvement over log binning. The advantage of soft binning is particularly pronounced when compared to hard binning: soft binning achieves a 41% improvement on SCIB metrics and a 92% improvement on macro F1 score over hard binning. Unlike hard binning, which loses information at bin boundaries, soft binning allows the model to express uncertainty and capture subtle differences between expression values. Unlike raw continuous encoding, soft binning provides some regularization and structure that may help the model learn more robust representations. The differentiable nature of soft binning also enables end-to-end training, allowing the bin assignments to adapt to the task.

Our evaluation is limited to human tissues, cell type classification, and a single model architecture. Results may differ for other species, disease conditions, or downstream tasks. Due to compute constraints, we did not perform hyperparameter search or ablation studies. Future research should evaluate additional downstream tasks and species, investigate alternative architectures, and provide mechanistic insights into why learned embeddings and soft binning outperform their alternatives.

7 CONCLUSION

We present a large-scale systematic benchmark comparing gene and expression encoding strategies for single-cell foundational models, training 8 configurations on over 10 million cells across 100 diverse datasets. Our evaluation using the scIB benchmarking framework (Luecken et al., 2022) yields three key findings.

First, task-specific learned gene embeddings substantially outperform ESM-2 transfer learning, achieving 29% improvement on SCIB metrics, 30% on classification accuracy, and 58% on macro F1 score (39% average improvement). This demonstrates that task-specific representations capture dataset-specific co-expression relationships more effectively than evolutionary protein-level information.

Second, soft binning emerges as the optimal expression encoding strategy when combined with learned gene embeddings, achieving 91.6% classification accuracy and 86.0% macro F1 score. This represents a 16% improvement over raw encoding on SCIB metrics and substantial gains over hard binning (41% on SCIB metrics, 92% on macro F1 score).

Third, gene encoding choice has greater impact than expression encoding choice, with learned embeddings providing consistent improvements across all expression encoding strategies. Our comprehensive evaluation establishes clear empirical guidance for model design decisions.

This benchmark provides reproducible results for future method development. Future work should explore hybrid approaches, evaluate additional downstream tasks and species, and provide mechanistic insights into why learned embeddings and soft binning outperform their alternatives.

IMPACT STATEMENT

This paper presents a benchmark study that provides empirical guidance for designing effective foundational models in single-cell RNA sequencing analysis. Potential positive impacts include enabling more effective analysis tools for biomedical research and providing reproducible benchmarks for method comparison. Potential negative impacts are limited, as this is a methodological study focused on model architecture rather than direct applications.

REFERENCES

Abhinav K Adduri, Dhruv Gautam, Beatrice Bevilacqua, Alishba Imran, Rohan Shah, Mohsen Naghipourfar, Noam Teyssier, Rajesh Ilango, Sanjay Nagaraj, Mingze Dong, Chiara Ricci-Tam, Christopher Carpenter, Vishvak Subramanyam, Aidan Winters, Sravya Tirukkova, Jeremy Sullivan, Brian S Plosky, Basak Eraslan, Nicholas D Youngblut, Jure Leskovec, Luke A Gilbert, Silvana Konermann, Patrick D Hsu, Alexander Dobin, Dave P Burke, Hani Goodarzi, and Yusuf H Roohani. Predicting cellular responses to perturbation across diverse contexts with state. *bioRxiv*, 2025. doi: 10.1101/2025.06.26.661135. URL <https://doi.org/10.1101/2025.06.26.661135>. Preprint.

Constantin Ahlmann-Eltze, Wolfgang Huber, and Simon Anders. Deep learning-based predictions of gene perturbation effects do not yet outperform simple linear methods. *Nature Methods*, 2024. doi: 10.1038/s41592-025-02772-6. URL <https://doi.org/10.1038/s41592-025-02772-6>. Published version.

Charlotte Bunne, Yusuf Roohani, Yanay Rosen, others, Emma Lundberg, Jure Leskovec, and Stephen R Quake. How to build the virtual cell with artificial intelligence: Priorities and opportunities. *Cell*, 187(25), 2024.

-
- Haotian Cui, Chloe Wang, Hassaan Maan, Kuan Pang, Fengning Luo, Nan Duan, and Bo Wang. sgcpt: toward building a foundation model for single-cell multi-omics using generative ai. *Nature Methods*, 21:1–12, 2024. doi: 10.1038/s41592-024-02201-0. URL <https://doi.org/10.1038/s41592-024-02201-0>.
- Shreshth Gandhi, Farnoosh Javadi, Valentine Svensson, Umair Khan, Matthew G. Jones, John Yu, Daniele Merico, Hani Goodarzi, and Nima Alidoust. Tahoe-x1: Scaling perturbation-trained single-cell foundation models to 3 billion parameters. *bioRxiv*, 2025. doi: 10.1101/2025.10.23.683759. URL <https://doi.org/10.1101/2025.10.23.683759>. Preprint.
- Ellie Haber, Shahul Alam, Nicholas Ho, Renming Liu, Evan Trop, Shaoheng Liang, Muyu Yang, Spencer Krieger, and Jian Ma. Heimdall: A modular framework for tokenization in single-cell foundation models. *bioRxiv*, pp. 2025–11, 2025.
- M. Hao, J. Gong, X. Zeng, et al. Large-scale foundation model on single-cell transcriptomics. *Nature Methods*, 21:1481–1491, 2024. doi: 10.1038/s41592-024-02305-7. URL <https://doi.org/10.1038/s41592-024-02305-7>.
- Nicholas Ho, Caleb N Ellington, Jinyu Hou, Sohan Addagudi, Shentong Mo, Tianhua Tao, Dian Li, Yonghao Zhuang, Hongyi Wang, Xingyi Cheng, Le Song, and Eric P Xing. Scaling dense representations for single cell with transcriptome-scale context. *bioRxiv*, 2024. doi: 10.1101/2024.11.28.625303. URL <https://doi.org/10.1101/2024.11.28.625303>. Preprint.
- Jared Kaplan, Sam McCandlish, Tom Henighan, Tom B. Brown, Benjamin Chess, Rewon Child, Scott Gray, Alec Radford, Jeffrey Wu, and Dario Amodei. Scaling laws for neural language models. *arXiv preprint arXiv:2001.08361*, 2020. URL <https://arxiv.org/abs/2001.08361>. Preprint.
- Zeming Lin, Halil Akin, Roshan Rao, Brian Hie, Zhongkai Zhu, Wenting Lu, Nikita Smetanin, Robert Verkuil, Ori Kabeli, Yaron Shmueli, Allan dos Santos Costa, Maryam Fazel-Zarandi, Tom Sercu, Salvatore Candido, and Alexander Rives. Evolutionary-scale prediction of protein structure from sequence. *Nature*, 622(7983):827–835, 2023. doi: 10.1038/s41586-023-06520-w. URL <https://doi.org/10.1038/s41586-023-06520-w>.
- Malte D. Luecken, M. Büttner, K. Chaichoompu, A. Danese, M. Interlandi, M. F. Mueller, D. C. Strobl, L. Zappia, M. Dugas, M. Colomé-Tatché, and Fabian J. Theis. Benchmarking atlas-level data integration in single-cell genomics. *Nature Methods*, 19:41–50, 2022. doi: 10.1038/s41592-021-01336-8. URL <https://doi.org/10.1038/s41592-021-01336-8>.
- James D Pearce, Sara E Simmonds, Gita Mahmoudabadi, Lakshmi Krishnan, Giovanni Palla, Ana-Maria Istrate, Alexander Tarashansky, Benjamin Nelson, Omar Valenzuela, Donghui Li, Stephen R Quake, and Theofanis Karaletsos. A cross-species generative cell atlas across 1.5 billion years of evolution: The transcriptformer single-cell model. *bioRxiv*, 2025. doi: 10.1101/2025.04.25.650731. URL <https://doi.org/10.1101/2025.04.25.650731>. Preprint.
- Yanay Rosen, Yusuf Roohani, Ayush Agarwal, Leon Samotorčan, Tabula Sapiens Consortium, Stephen R Quake, and Jure Leskovec. Universal cell embeddings: A foundation model for cell biology. *bioRxiv*, 2023. doi: 10.1101/2023.11.28.568918. URL <https://doi.org/10.1101/2023.11.28.568918>. Preprint.
- Tabula Sapiens Consortium, Robert C Jones, Jim Karkanias, Mark A Krasnow, Angela Oliveira Pisco, Stephen R Quake, Julia Salzman, Nir Yosef, Bryan Bulthaup, Phillip Brown, Will Harper, Michael Hemenez, Ravikumar Ponnusamy, Ahmad Salehi, Bhavani A Sanagavarapu, Eileen Spallino, Kalleen A Aaron, Waldo Concepcion, James M Gardner, Brendan Kelly, Nicholas Neidlinger, Zifa Wang, Sheela Crasta, Saroja Kolluru, Maurizio Morri, Yan Tan, Kyle J Travaglini, Chenling Xu, Maria Alimova, Nicholas E Banovich, Ben A Barres, Philip A Beachy, Biter Bilen, Douglas Brownfield, Charles K F Chan, Songming Chen, Michael F Clarke, Sabrina D Conley, Spyros Darmanis, Aaron Demers, Kubilay Demir, Antoine de Morree, Tony Divita, Haley du Bois, Hamid Ebadi, F Hernan Espinoza, Matt Fish, Qiang Gan, Benson M George, Jeffrey M Granja, Foad Green, Gunsagar S Gulati, Michael S Haney, Julie A Harris, Yanzhe He, Shayan Hosseinzadeh, Albin Huang, Kerwyn Casey Huang, Atsushi Iriki, Eric Jean, Kevin S

Kao, Guruswamy Karnam, Aaron M Kershner, Bernhard M Kiss, William Kong, Maya E Kumar, Jonathan Lam, Song E Lee, Benoit Lehallier, Qiang Li, Yan Li, Ling Liu, Annie Lo, Wan-Jin Lu, Marisol F Lugo-Fagundo, Anjali Manjunath, Andrew P May, Ashley Maynard, Aaron McGeever, Madeleine McKay, Michael I Miller, Mais Moussa, Ravi Mylvaganam, EK Neumann, Joseph Noh, Roel Nusse, Irene Papatheodorou, Traci Peng, Lolita Penland, Katherine Pollard, Robert Puccinelli, Zhen Qi, Stephen R Quake, Thomas A Rando, Micha Sam Raredon, Karine Rizzoti, Katherine Rogers, Yanay Rosen, M Elizabeth Rothenberg, Meritxell Rovira, Yaroslava Ruzankina, Nicholas Schaum, Eran Segal, Jun Seita, Rahul Sinha, Rene V Sit, Justin Sonnenburg, Christof Stringer, Kai Tan, Michelle Tan, Sudhir Gopal Tattikota, Kyle J Travaglini, Carolina Tropini, Michelle Tsui, Lucas Waldburger, Bruce M Wang, Linda J van Weele, Brice M Weinstein, Michael N Wosczyna, Angela Wu, Jinyi Xiang, Sizun Xue, Kevin A Yamauchi, Andrew C Yang, Lakshmi P Yerra, Justin Youngyunpipatkul, Bo Yu, Fabio Zanini, Gizem Zardeneta, Tiffany Zee, Chunyu Zhao, Fan Zhang, Hui Zhang, Martin Jinye Zhang, Lu Zhou, and Daniel R Zollinger. The tabula sapiens: A multiple-organ, single-cell transcriptomic atlas of humans. *Science*, 376(6594):eabl4896, 2022. doi: 10.1126/science.abl4896. URL <https://doi.org/10.1126/science.abl4896>.

Christina V Theodoris, Ling Xiao, Anant Chopra, Mark D Chaffin, Zeina R Al Sayed, Matthew C Hill, Helene Mantineo, Elizabeth M Brydon, Zexian Zeng, X. Shirley Liu, and Patrick T Ellinor. Transfer learning enables predictions in network biology. *Nature*, 618(7965):616–624, 2023. doi: 10.1038/s41586-023-06139-9. URL <https://doi.org/10.1038/s41586-023-06139-9>.

Ashish Vaswani, Noam Shazeer, Niki Parmar, Jakob Uszkoreit, Llion Jones, Aidan N Gomez, Łukasz Kaiser, and Illia Polosukhin. Attention is all you need. *Advances in Neural Information Processing Systems*, 30, 2017. URL <https://proceedings.neurips.cc/paper/2017/file/3f5ee243547dee91fb053c1c4a845aa-Paper.pdf>.

Wenchuan Wang, Fan Yang, Yuan Fang, Duyu Tang, Junzhou Huang, Hui Lu, and Jianhua Yao. scbert: a large-scale pretrained deep language model for cell type annotation of single-cell rna-seq data. *bioRxiv*, 2021. doi: 10.1101/2021.12.05.471261. URL <https://doi.org/10.1101/2021.12.05.471261>. Preprint.

A. Wenteler, M. Occhetta, N. Branson, M. Huebner, V. Curean, W. T. Dee, W. T. Connell, A. Hawkins-Hooker, S. P. Chung, Y. Ektefaie, A. Gallagher-Syed, and C. M. V. Córdova. Perteval-scfm: Benchmarking single-cell foundation models for perturbation effect prediction. *bioRxiv*, 2024. doi: 10.1101/2024.10.02.616248. URL <https://doi.org/10.1101/2024.10.02.616248>. Preprint.

A ADDITIONAL DETAILS

A.1 REPRODUCIBILITY

Training datasets are from publicly available sources (Pearce et al., 2025). Evaluation datasets from Tabula Sapiens v2 are available from the official repository (Tabula Sapiens Consortium et al., 2022).

A.2 HYPERPARAMETERS

Table 1 summarizes the hyperparameters used for training all models in this study.

A.3 TRAINING DATASETS

Table 2 lists all 101 training datasets used in this study, including the dataset identifier and number of cells for each dataset. The total number of cells across all training datasets is 10,010,835.

A.4 ADDITIONAL FIGURES

Table 1: Hyperparameters used for model training.

Hyperparameter	Value
<i>Model Architecture</i>	
Model dimension (d_{model})	512
Number of transformer blocks (n_{blocks})	12
Number of attention heads (n_{head})	8
Feed-forward dimension (d_{hid})	1024
Dropout	0.1
Context window	1024
<i>Training</i>	
Batch size	512
Gradient accumulation steps	32
Effective batch size	16,384
Epochs	3
Learning rate	3×10^{-4}
Weight decay	10^{-5}
Optimizer betas	[0.9, 0.95]
Max gradient norm	1.0
Scheduler	Cosine annealing
Warmup steps	2000
Early stopping patience	100
<i>Data</i>	
Validation ratio	0.001
Test ratio	0.001
Masking probability (p_{mask})	0.5
<i>Expression Encoding</i>	
Raw hidden dimension	512
Hard binning bins	50
Soft binning bins	20
Soft binning hidden dimension	512
Log binning max bins	10
<i>Other</i>	
Random seed	777
Number of data workers	8

Table 2: Training datasets used for model pretraining. Dataset IDs are UUIDs from the curated dataset collection.

Dataset ID	Cells	Dataset ID	Cells	Dataset ID	Cells
7d98cc44-b090-4dc8-804f-2750c84fe9d7	2,489	2f05ab20-a092-4bab-9276-3e0eb24e3fee	38,217	3966ba97-beb8-4d0b-9954-d3775cd2cd61	158,978
2d66790a-6621-4a49-f8fd-4002db5cc98d	4,992	76150f40-1989-4977-9c23-696e72d59d9e	118,672	28ab6eb8-dfa4-4536-9f26-7e06c1b98e8e	25,741
50c4a6d6-940b-4c6a-a376-aee2ae2d3168	21,003	c2a461b1-0c15-4047-9fcf-1966fe55100	97,499	c838aec3-03ef-4398-b882-0e3912abff0	1,265,624
cda2c8cd-be1c-42e5-b2cd-162caa1c4ce7	255,901	e40c6272-af77-4a10-9385-62a398884f27	65,088	3a29c3df-b45a-403d-bd76-259640245432	4,992
19e46756-9100-4e01-8b0e-23b557558a4c	66,985	ed11cc3a-2947-407c-883c-c53b0e3917c3	8,573	61d327d1-2227-4cf6-9367-e3559dc79b07	796
70e4f35b-c98c-45a1-9aa1-2053b07315d4	40,815	15327a6-7978-4896-ba91-69d6b402dbbf	40,191	eeac8bc1-2217-4cf6-b8ce-1f0fedfb1b569	9,337
c5ac3ec2-24b0-43cc-9aa8-bb0ebe205ce	4,992	a6046b15-a095-43b0-9fb5-b36989d87fdb	4,992	0fe5eed4-bcbc-4c00-a388-00bc1455a9b7	4,992
bac09168-940b-4b11-8d55-b495f80b98d	12,461	9fcfac8d-bff6-47a2-a1f6-503827d375f5	637	43aa19d2-c723-4822-979d-d2f0239835e0	37,121
095940cb-7422-4510-96e2-cba9d961eb88	52,045	30f5e171-83d7-4fc0-bf75-384f122346b3	1,790	3079e9b0-c6db-45c8-b998-a4555a73968e	28,943
79884ac5-e026-4d44-8585-e807960bd477	4,425	489318a0-24c3-4fc5-b105-08f4ed0ea026	13,900	0920cb8c-4b3a-4e9d-a553-561529fd3b32	48,478
d551b400-b2e5-454d-b5a9-ece03e6b4739	4,992	a7b4f565-691d-43ea-bf4a-d2d1d52b4b4	27,111	93091496-be48-4122-b945-9a9c227535	28,718
b9b592d4-a0c0-4694-a704-a625289ef1f	4,992	34229bd8-a954-4394-8820-574e028d8c6	31,924	01209dce-3575-4bed-b1d1-129f571bc031	51,876
311657dc-1875-4c4b-a5ca-ce63b3ef3a82	121,916	e5f5d954-cf0e-4b8d-9346-81ddf15a08b	2,487	879bb6df-cc2a-40f1-854b-5be9629d03b2	4,992
edbfa04a-f1dd-496a-8237-df11d70621ca	77,525	6e6f6b36-6c9b-4e10-8a94-d0ba7247276e	10,533	79527108-1f6c-4152-afe0-1fcdf2e02ba3	4,992
f60f858c0-c590-4740-b022-c152e7608d66	4,992	9ea768a2-87ab-46b6-a73d-c4e9152f5af3	40,268	dee75ca4-8348-471e-bbeb-e2143209e3d0	4,992
949e7fc-ac54-47e9-bb6f-ee967688ce	38,937	0bae7ebf-eb54-4f6b-be9a-3461ceef4ac	27,675	1df5fa02-4a0e-4b00-a203-cb0a60e75637	4,992
7291f397a-0812-4b52-a7d1-b377107ffb41	4,992	53d62b10-bae5-48ac-b16c-71be9bafde59	4,992	364bd0e7-f7fd-48ed-99c1-ac26872b1042	931,012
ae4552dc-e2ea-44d7-b375-30ec7480f780	37,275	fe2479fd-daff-41a8-97dc-a50457ab1871	292,010	50eb1e23-b8d4-4f76-a184-44e55416a05a	4,775
77c1c78-8094-4065-8c34-6a070783256	37,767	49108a9b-1b7a-4a8a-9859-3d3e0ba3926	4,992	39ed7d98-676d-4b8d-9d0d-0f3b60914ead	118,647
dd03ce70-3243-4c96-5961-330cc4164d7	23,732	00ba8341-48ec-4b5e-4a0d-00dd2d7913	4,992	9ddea8d9-c4c4-420a-90f6-880996808d4	100,307
9dbab10c-118a-496b-966a-671f763a6b7d	1,462,702	ca421096-6240-4cce-8c12-d20899b3e005	81,736	731e6380-879f-4b0b-9a1f-2150208852ef	2,065
43245158-5ae1-4e71-a9a6-67ef49c26bc	113,304	f801b7a9-80a4-6d09-9161-71474deb58a	6,044	54801477-ac3e-47e3-8170-96c5b40d5c10	4,992
43848156-ba94-47b5-8409-7535cea75678	4,992	c5ca2b7-abb1-4a50-9087-707b54ca606b	14,094	1cf24082-59de-4029-ac81-6e398768af3a	29,522
978a566a-dc27-478d-b306-26dab1161f	1,102,250	726afad9-df7b-4b56-967a-0fb79d85ee4b	4,992	9ad81b29-65a2-4dd0-86bf-f02690d65fb	4,992
e6361237-ac4e-4c5d-ad8f-f16aca0c0a8f1	66,719	344f27ab-428c-4a0e-a7e1-d4441f29fb80	4,992	a8b241a-c72c-4470-b1a4-80e7336c6ab6	4,335
346c5aad-b034-4248-8c8e-0a05fd634b9c	163,779	529b209-9d7b-44da-bfa4-f6e4745c46c2	32,678	33da10b0-9c1d-4c82-9b14-67cdcf9fae5	30,022
d98e49fe-b70d-4434-8050-bb179b66e	15,216	5e57cd50-8e42-42d6-940d-5c1660d06864	693,682	3e55180c-780a-4424-9434-5296640fc0d	7,774
f3c49918-4707-4d92-bb6d-5e5231b1b4	15,177	c5cd6bbb-8ba4-4338-8b34-51ed5b231e2	4,992	b617ee1b-18c8-4d89-b82b-e803ab93550d	391,963
9f499d32-400d-4c42-a9a2-fb1481844fe	56,367	93131426-0124-4a04-ba13-9dfb99d467	24,327	ab8896c6-f60a-51ef-b924-e1-ee9dcf909b	4,992
2f6a4db1-173d-4b8d-860b-47fea120fa	2,868	75548d10-160d-4c3e-b317-99ad9630c62d	4,992	e84f2780-518c-4fca-8a0-13bfe6f77c7	167,598
be401db3-732-408a-b0c4-71af0458bab	135,462	6e92c3624-02e1-455a-840b-4bcee132ae7	4,992	639ffcc23-14db-4060-9027-3c903142008	35,290
4724c395-0c46-46d2-8117-60fd271fb488	35,350	4f2de279-ab3a-4827-a773-1b7dcd099307	4,992	c775e88-49bf-4ba2-a03b-93f00447c958	647,366
155c186-df92-4b17-a253-199e10ffea08	4,992	019e7af2-c827-4454-9970-44d5c39ce068	12,590	842cf0d-0b0a-46d5-910c-fc833d83c45e	65,662
1b767195-d0a-43ad-b394-cc665d86c3dc	34,933	b3c55d0d-4529-4b61-b485-29026be04e	4,992		

Total: 10,010,835

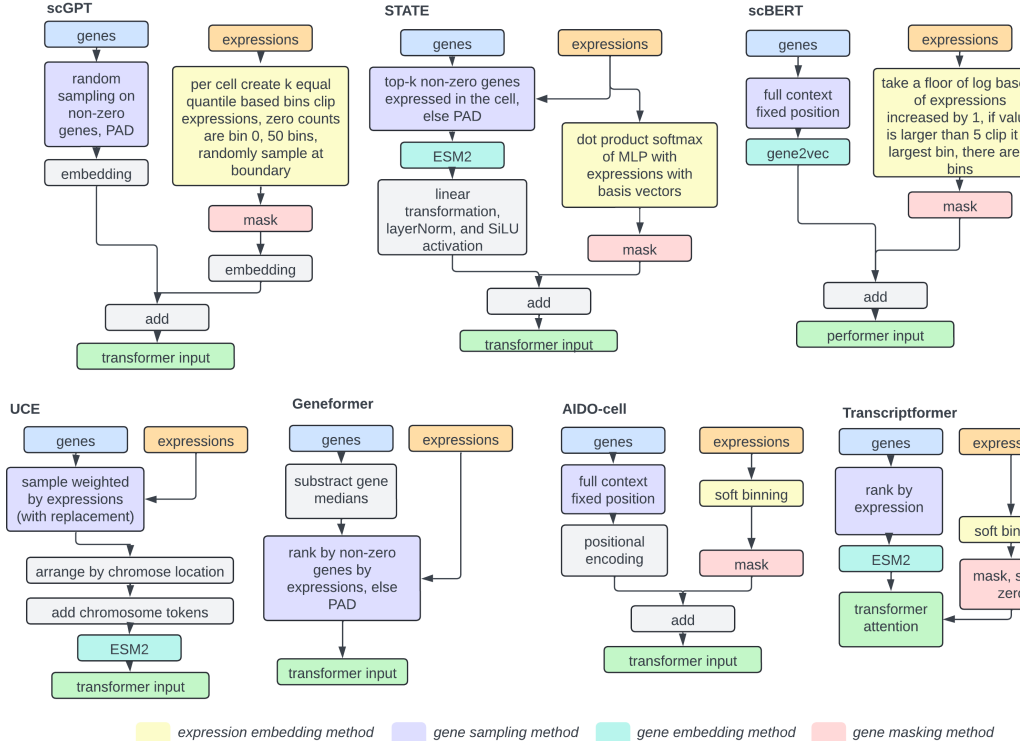


Figure 4: Schematic comparison of different gene and expression encoding methods across single cell foundational models (Cui et al., 2024; Adduri et al., 2025; Ho et al., 2024; Wang et al., 2021; Theodoris et al., 2023; Pearce et al., 2025; Rosen et al., 2023).